ELSEVIER

Earth and Planetary Science Letters 198 (2002) 41–48

EPSL

www.elsevier.com/locate/epsl

GPS deformation in a region of high crustal seismicity: N. Cascadia forearc

Stéphane Mazzotti [a,b,*], Herb Dragert [b], Roy D. Hyndman [a,b], M. Meghan Miller [c], Joseph A. Henton [a,b]

[a] *School of Earth and Ocean Sciences, University of Victoria, P.O. Box 3055, STN CSC, Victoria, BC, Canada V8W 3P6*
[b] *Pacific Geoscience Centre, Geological Survey of Canada, 9860 W. Saanich Rd., Sidney, BC, Canada V8L 4B2*
[c] *Department of Geological Sciences, Central Washington University, Ellensburg, WA 98926 USA*

Received 20 August 2001; received in revised form 11 December 2001; accepted 5 February 2002

Abstract

We estimate the rate of crustal deformation in the central and northern Cascadia forearc based on a combination of existing global positioning system (GPS) velocity data along the Cascadia subduction zone. GPS strain rates and velocities show that the northwestern Washington–southwestern British Columbia region is currently shortening at 3–3.5 mm yr^{-1} in a N–S direction, in good agreement with inference from crustal earthquake statistics. On the long-term, the shortening rate is 5–6 mm yr^{-1}, providing that the subduction-related interseismic loading of the margin is purely elastic. Compared to the velocity of the Oregon forearc with respect to North America ($\sim$7 mm yr^{-1}), this indicates that most of the forearc motion is accommodated in the Puget–Georgia basin area, corresponding to the main concentration of crustal seismicity. The difference between the current and long-term shortening rates may be taken up during subduction megathrust earthquakes. Thus, these events could produce a sudden increase of N–S compression in the Puget sound region and could trigger major Seattle-fault-type crustal earthquakes. Published by Elsevier Science B.V.

Keywords: deformation; Cascadia subduction zone; fore-arc basins; Global Positioning System; seismicity

1. Introduction

Along the Cascadia margin, the Juan de Fuca (JF) plate subducts obliquely beneath the North American (NA) plate (Fig. 1). As in many other oblique subduction zones (e.g., SW Japan, Philippines Arc), the Cascadia margin is affected by the margin-parallel migration of a forearc sliver, the Oregon (OR) block. Models of rigid block kinematics suggest that the OR/NA velocity ranges between $\sim$15 mm yr^{-1} toward NW and $\sim$7 mm yr^{-1} toward NNE, from southern to northern Oregon [1,2]. Long-term shortening is a common feature of the leading edge of forearc slivers. In the Cascadia forearc, N–S deformation is documented in the Puget Sound–Georgia Basin region by crustal earthquakes and active thrust faults [3,4].

In this study, we formally combine global posi-

* Corresponding author. Tel.: +1-250-363-6451; Fax: +1-250-363-6565.
E-mail address: mazzotti@pgc.nrcan.gc.ca (S. Mazzotti).

0012-821X/02/$ – see front matter Published by Elsevier Science B.V.
PII: S0012-821X(02)00520-4

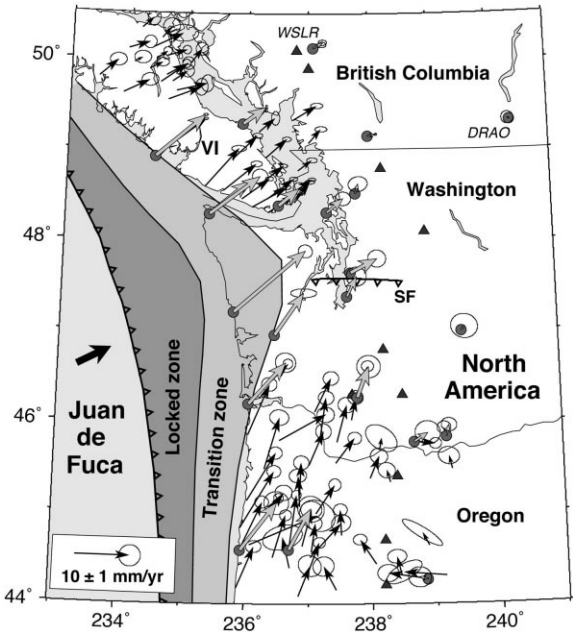

Fig. 1. GPS velocity data in northern Cascadia. GPS velocities, with respect to station DRAO, are show by thin solid arrows (campaign sites) and large shaded arrows (permanent sites). Solid lines represent, from west to east, the subduction front, the downdip ends of the locked and transition zones of the subduction thrust. VI: Vancouver Island; SF: Seattle fault.

tioning system (GPS) velocity data along the Cascadia margin to determine the location and rate of the current and long-term N–S shortening associated with the forearc migration. Long-term deformation rates are obtained by removing from the GPS data the predicted interseismic deformation associated with the megathrust earthquake cycle. The combined GPS velocity field shows that N–S shortening occurs primarily in the Puget Sound–south Georgia Basin, in agreement with the concentration of crustal seismicity, but also in the Olympic Mountains where very little seismicity is observed.

Recent studies along different convergent margins have shown that a proper modeling of the transient and long-term components of GPS velocities can provide useful constraints on the tectonics and seismicity of the forearc (e.g. [5,6]). In northern Cascadia, the significant difference between the current and long-term shortening rates could have important implications for seismic hazard assessment. Based on our estimates, we discuss the possible effect of subduction megathrust events on large crustal earthquake recurrence rates and their possible interaction.

2. GPS velocities

The Pacific Northwest Geodetic Array (PANGA) in Oregon and Washington [7] and the Western Canada Deformation Array (WCDA) in British Columbia [8] consist of 28 permanent GPS stations in operation from 2 to 7 yr (Fig. 1). Campaign GPS surveys covering Vancouver Island [9] and Oregon [2] contribute to the densification of the data set. Velocities derived from these networks are divided into three groups on the basis of their reference system: (1) The PANGA solution is referenced to NA based its own definition of the NA/ITRF97 rotation vector [7]; (2) The Oregon solution is referenced to NA based on the DeMets and Dixon (1999) NA/ITRF96 rotation vector [10]; (3) The WCDA and Vancouver Island solutions are referenced to the station DRAO (Penticton, BC, Canada) and corrected for the NA differential motion between DRAO and each GPS station using the PANGA NA/ITRF97 pole [7].

In order to interpret these data in terms of forearc deformation, we combine them into a common reference system. We first adjust the Oregon network velocities to the PANGA solution in three steps: (1) The Oregon solution is mapped back from NA to ITRF96, using the NA/ITRF96 rotation vector [10]; (2) It is formally transformed from ITRF96 to ITRF97, using a full Helmert transformation based on a comparison of the ITRF96 and ITRF97 solutions at the 51 GPS reference stations (M. Craymer, personal communication, 2001); (3) The Oregon solution is mapped in the NA reference frame using the PANGA NA/ITRF97 rotation vector [7]. This set of transformations leads to small velocity corrections of the Oregon solution of (0.3–0.5) ± (0.4–0.5) mm yr^{-1}. The consistency of the combined PANGA–Oregon solution is indicated by the small (0.63 mm yr^{-1}) root-mean-square velocity difference at eight common sites.

In a second phase, we adjust the combined PANGA–Oregon solution to the WCDA–Vancouver Island solution to obtain a final global solution referenced to the station DRAO. We estimate the velocity differences between the PANGA and WCDA solutions at seven common sites (between 48 and 52°N) and solve for a rigid rotation best fitting those vectors. Because the best fit rotation pole is located in the Gulf of Mexico ~4000 km SE of the Cascadia region, this transformation is close to a simple north–northeast translation of 1.5–2.0 (±0.6) mm yr^{-1}. The root-mean-square residual between the transformed PANGA velocities and the WCDA velocities at the common sites is 0.48 mm yr^{-1}, indicating a good agreement between the final solutions. The uncertainties associated with these different transformations are formally propagated to the combined GPS velocities.

3. Model of subduction interseismic loading

Numerous studies have shown that the Cascadia subduction thrust is currently locked, leading to an accumulation of interseismic strain along the upper plate margin (e.g. [11,12]). In order to obtain long-term velocity and strain fields associated with the Oregon forearc motion, it is necessary to account for this transient deformation. We estimate the subduction interseismic loading using a standard model of back-slip dislocation within an elastic medium [13]. The geometry and the extent of the locked and transition zones of the subduction thrust (Fig. 1) are based on seismic, thermal, and geodetic constraints [12]. The precise 3D structure is modeled using a point-source discretization of the fault [14]. We assume that the coupling coefficient is 1 on the locked part of the subduction thrust and that it decreases linearly from 1 to 0 on the transition zone downdip from the lower end of the locked zone.

The convergence velocity between the subducting plate and the forearc is controlled by the JF/NA rotation vector and is corrected for the forearc motion with respect to NA. We define the JF/NA rotation vector as the sum of the PA/NA vector [10] and the JF/PA vector at 0.78 Myr [15]. This new JF/NA vector (35.3°N, 243.0°E, −1.45°/Myr) predicts a more oblique subduction velocity (by 10–20°) and a stronger along-strike gradient of convergence compared to the NUVEL-1A JF/NA pole averaged over 3 Myr [16].

The convergence velocity vectors predicted by this JF/NA rotation pole are then corrected for the forearc motion using an iterative approach. First, the predicted interseismic subduction-loading velocity field is removed from the GPS velocities to obtain the long-term residual OR/NA motion at every station. These GPS velocities are averaged over the forearc width along 50 km latitude slices to estimate a N–S profile of the forearc velocity, which is then used to correct the convergence velocity vectors. The new convergence vectors produce a new interseismic subduction-loading deformation field, new residual velocities at the GPS stations, and a new long-term forearc velocity profile. A stable model of convergence velocities and average forearc motion is obtained after two iterations of this procedure. Fig. 2 shows the final convergence model, the predicted subduction-loading interseismic velocities at the GPS sites, and the residual GPS velocities along the Cascadia margin.

4. GPS strain rates and subduction-related deformation

In order to study the along-strike variation of forearc deformation, we estimate strain rates from central Oregon to central Vancouver Island based on the original GPS velocities (not corrected for subduction interseismic deformation), and we compare them with strain rates derived from the predicted interseismic velocity field (Fig. 2). The strain rate tensors are averaged over the forearc width within a region ~150 by 150 km using exclusively GPS velocities of the same network solution. Thus, they are not affected by our reference frame adjustments. Assuming uniform deformation of the area of interest, the tensors are computed by fitting a 2D linear function to a set of 6–15 GPS velocities, depending on the region.

The GPS strain rates standard deviation ranges

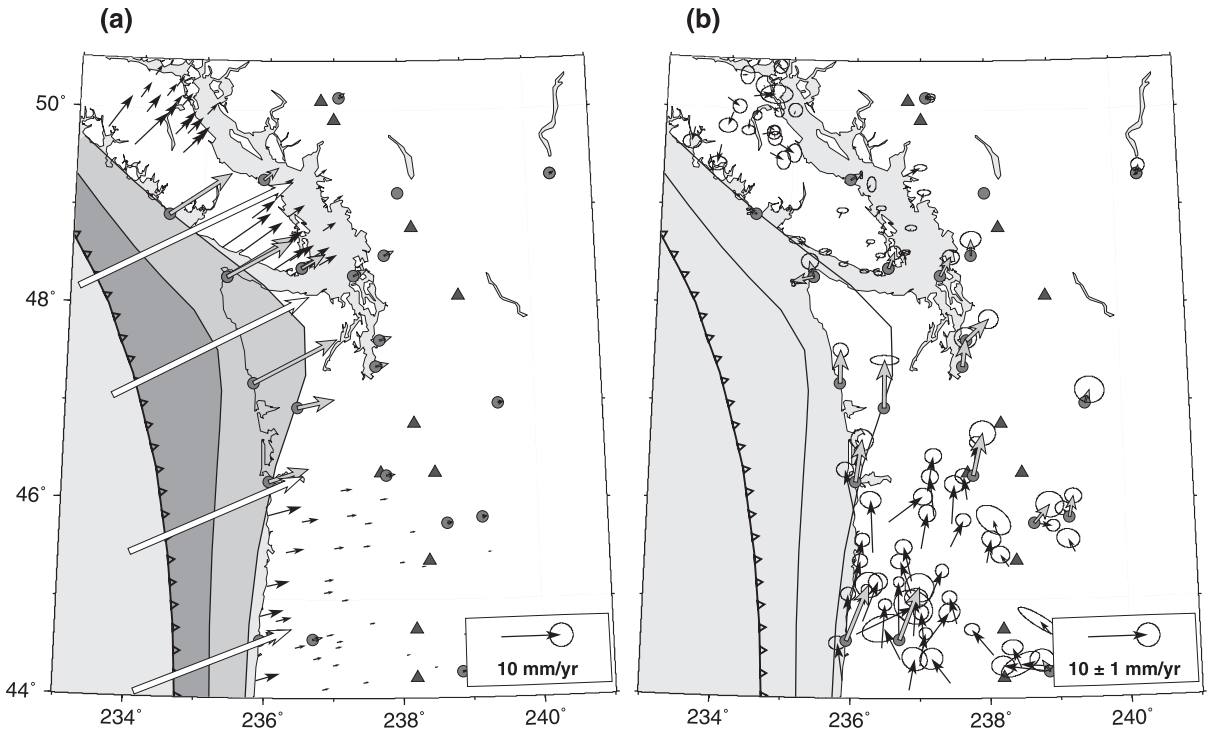

Fig. 2. Interseismic and long-term velocities. (a) Interseismic subduction-loading velocities at the GPS sites (solid and shaded arrows) predicted by our convergence model (white arrows). (b) Residual GPS velocities at permanent (shaded) and campaign (solid) sites after correction for the interseismic deformation shown in (a).

between 5×10^{-9} and 20×10^{-9} yr^{-1} for magnitude and between 1 and 5° for principal axis direction. They indicate mostly uniaxial shortening between 40×10^{-9} and 80×10^{-9} yr^{-1} (Fig. 3). The shortening direction is nearly E–W in central and northern Oregon; it progressively rotates counter-clockwise northward and becomes nearly NE–SW in southern coastal British Columbia.

In Oregon, southern Washington and southern Vancouver Island, the observed strain rates are consistent in direction and, to a first order, in magnitude with those predicted by the subduction-loading model. However, in northwestern Washington the GPS shortening direction shows a significant counter-clockwise rotation with respect to that predicted (Fig. 3). This rotation increases eastward: along the coast, the GPS strain rate direction differs by $\sim$10° with the model, whereas it differs by $\sim$30° along the inner forearc.

Thus, GPS strain rates indicate that the northern Washington forearc is affected by significant N–S shortening as well as margin-normal interseismic subduction loading. This last component alone can account for the deformation observed along the Oregon and Vancouver forearc. This strain pattern is consistent with Oregon forearc migration as a relatively rigid block ending at 46–47°N.

5. Shortening across the Puget–Georgia basin

The current sparse coverage of GPS stations allows only for a first-order separation of transient strain due to the locked subduction thrust from permanent strain associated with steady N–S tectonic stress. Strain partitioning is addressed by examining the margin-parallel variations of the northward component of the GPS velocities. We divide the GPS data into an inner (eastern) forearc and an outer (western) forearc

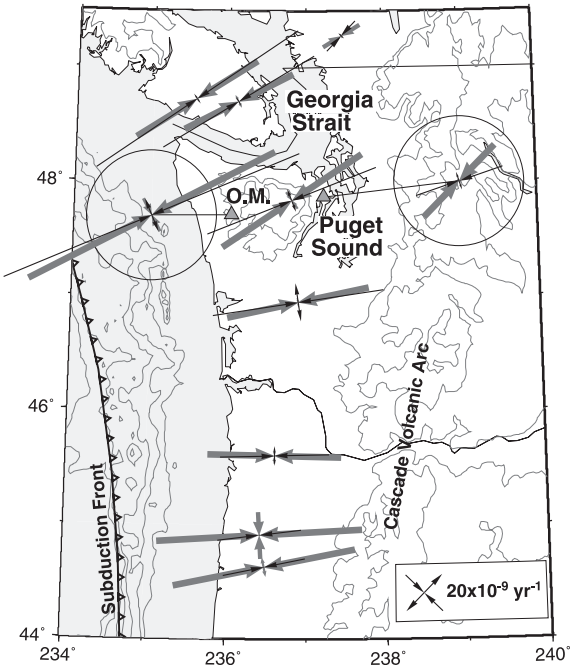

Fig. 3. GPS versus model strain rates. Large shaded and thin solid arrows represent the principal axes of GPS and interseismic model strain rates averaged over $\sim 150 \times 150$ km. Strain arrows within circles represent strain rates estimated in the western and eastern sides of the northern Washington forearc (shaded triangles indicate the center of those two regions). O.M.: Olympic Mountains.

set. This separation follows the half-width line of the forearc, with a small overlap of 40 km between the two regions.

In northern Oregon–southern Washington, the inner and the outer forearc northward velocities are ~ 6 and ~ 8 mm yr^{-1}, respectively (Fig. 4). These estimates are in agreement with the predicted velocity of the Oregon sliver relative to NA from geologic [1] and GPS [2] data at 46°N. The differential northward motion between southern Washington and southern Vancouver Island is 3.0 ± 0.7 mm yr^{-1} in the inner part of the forearc and 3.4 ± 0.8 mm yr^{-1} in the outer part (Fig. 4; Table 1). This corresponds to N–S shortening of $\sim 15 \times 10^{-9}$ yr^{-1} across the ~ 200 km long region of the Puget Sound and Olympic Mountains. This location is in good agreement with the concentration of crustal seismicity in the Puget–Georgia region (Fig. 5).

Velocities measured by GPS consist of a transient, megathrust interseismic loading part and a long-term, steady forearc tectonics part. The north component of the predicted subduction-loading velocity is shown in Fig. 4. In Oregon, this signal is small, from 1–3 mm yr^{-1} along the coast to < 1 mm yr^{-1} in the inner forearc. Because it is located closer to the subduction thrust locked zone, the northern Washington–southern Vancouver Island forearc loading has a larger north component (3–8 mm yr^{-1}) that increases to the north. Thus, between northern Oregon and southern British Columbia the modeled interseismic subduction-loading corresponds to N–S extension varying from 1–2 mm yr^{-1} along the inner forearc to 3–4 mm yr^{-1} along the outer side.

If we assume that the subduction-related interseismic deformation is totally elastic, we can subtract this deformation from the GPS data and interpret the residual in terms of long-term forearc average motion (Figs. 2b and 4). The along-strike variation of the residual north velocities is similar to that of the original GPS data. Because the elastic N–S extension associated with the megathrust earthquake cycle was removed, the long-term N–S shortening between southern Washington and southern Vancouver Island increases to 4.8 ± 0.6 mm yr^{-1} in the inner forearc and 6.5 ± 0.7 mm yr^{-1} in the outer forearc (Table 1).

These values are based on our assumptions of a full coupling along given subduction thrust locked and transition zones. A recent study suggests that, because of the viscous relaxation of the upper mantle after the last subduction earthquake, the transition zone could currently extend inland twice as far, with a non-linear decrease of the coupling coefficient [17]. This model predicts a smaller landward decrease of the interseismic deformation, but has little effect on the northward component of the predicted interseismic and re-

Table 1
N–S shortening in northern Cascadia

	Inner (E) forearc mm yr^{-1}	Outer (W) forearc mm yr^{-1}
Current	3.0 ± 0.7	3.4 ± 0.8
Long-term	4.8 ± 0.6	6.5 ± 0.7

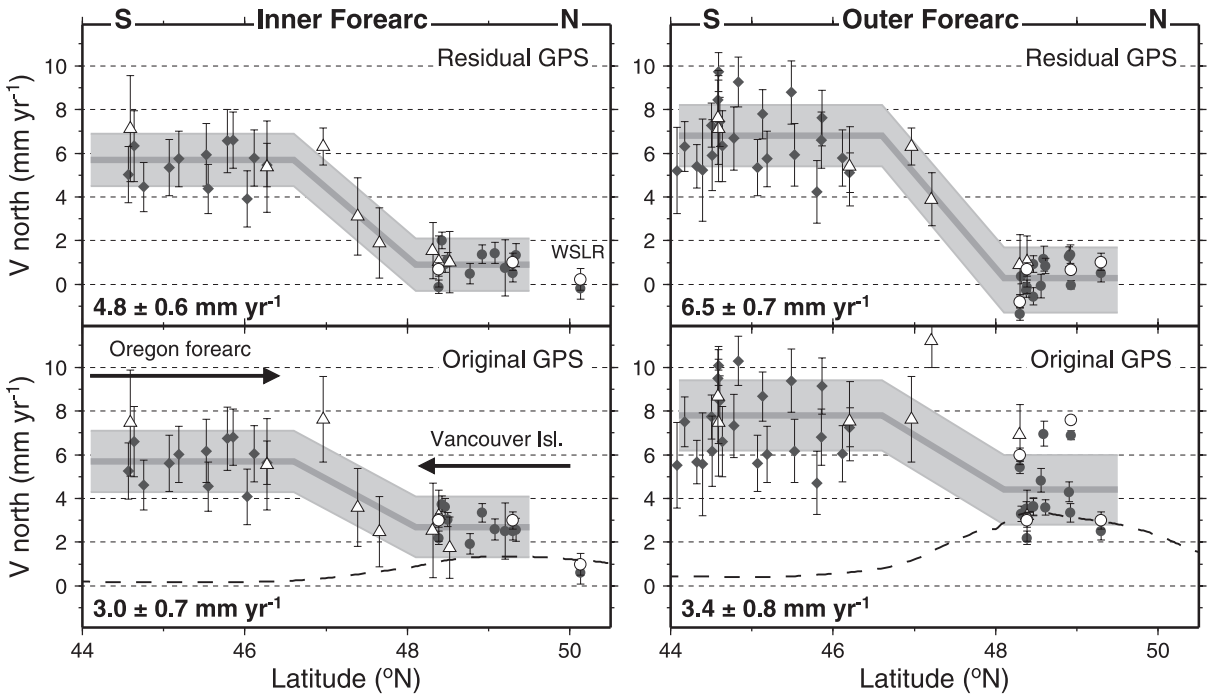

Fig. 4. North component of original and residual GPS velocities. Shaded diamonds, shaded circles, open triangles and open circles represent the Oregon campaign, Southern Vancouver Island campaign, PANGA and WCDA velocities with respect to the station DRAO (error bars at 95% confidence level). Dashed lines show the north component of the predicted interseismic subduction signal along the inner and outer forearc profiles.

sidual GPS velocities. Thus, our estimates of the long-term N–S shortening are close to upper bound values.

These long-term shortening rates, based on a combination of GPS solutions along the central and northern Cascadia margin, are larger than a previous estimate ($\sim$4 mm yr^{-1}) based on the analysis of much more limited PANGA data in western Washington [18]. Our combined GPS velocity field allows us to discriminate between the inner and outer forearc, suggesting a westward increase of the shortening in the Washington, in agreement with the location the OR/NA rotation pole in the Columbia basin.

6. Discussion

The combined GPS velocity data along the Cascadia margin are now sufficient in quality and number to show that the forearc region between northern Washington and the southernmost Vancouver Island is currently undergoing significant N–S shortening at 3–3.5 mm yr^{-1}, in relation with the northward migration of the Oregon sliver. This current GPS N–S shortening rate agrees well with the rate derived from crustal earthquake statistics in the Puget–Georgia basin region (2–3 mm yr^{-1} [19]). The lack of seismicity in the Olympic Mountains (Fig. 5) suggest that the shortening indicated by GPS data is accommodated by ductile deformation in the sedimentary core rocks that appear to extend down to the subducting plate.

The residual GPS velocities (after subtraction of the subduction-related interseismic loading) show a larger long-term N–S shortening rate of 5–6.5 mm yr^{-1}, in general agreement with the estimation based on Neogene fault motions ($\sim$4 mm yr^{-1} for the last 15 Myr [20]). Compared to the predicted OR/NA motion ($\sim$7 mm yr^{-1}), the GPS-derived N–S shortening rate indicates that

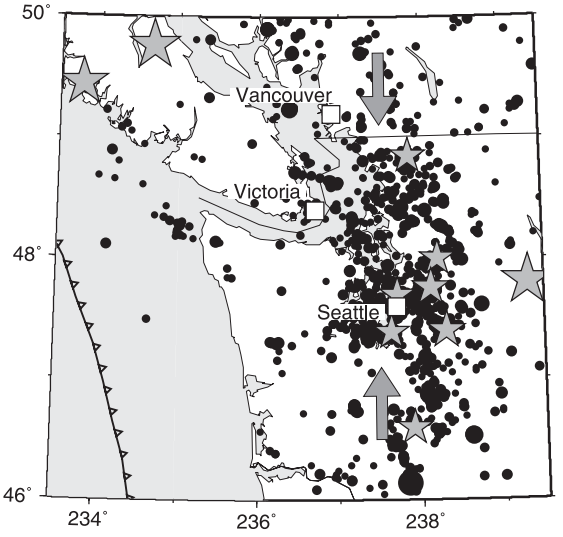

Fig. 5. Crustal seismicity in northern Cascadia. Solid circles represent shallow earthquakes (depth≤30 km, M≥2) between 1980 and 2000. Shaded stars show crustal M≥5 earthquakes since 1872.

most of the Oregon forearc migration is accommodated in the Puget–Georgia basin and Olympic Mountains region. A small part (1–2 mm yr^{-1}) is accommodated either to the south in the Oregon forearc [21] or to the north in the central Georgia Basin and the southernmost Canadian Coast Mountains. This last hypothesis is supported by: (1) the residual GPS velocities that indicate a northward motion of 1 ± 0.3 mm yr^{-1} of southern Vancouver Island with respect to the Coast Mountains (stations WSLR, Fig. 4); and (2) crustal seismicity to the north of the main concentration area (Fig. 5), with focal mechanisms consistent with N–S compression.

This study of N–S shortening across the Puget–Georgia basin area leads to an interesting conclusion on seismic occurrence. The N–S component of the subduction-related interseismic deformation corresponds along the inner forearc to 1–2 mm yr^{-1} of extension between the southern Washington and southern Vancouver Island. If this elastic deformation is totally released during a megathrust earthquake, and assuming 500 yr of recurrence for subduction events, there should be an abrupt N–S shortening in the Puget–Georgia basin of 0.5–1 m (Fig. 6). This sudden strain could lead to an increase in crustal earthquake activity in the area and could trigger large Seattle-fault-type earthquakes shortly after the subduction event.

To illustrate this possible interaction between a subduction earthquake and the forearc seismicity, we calculate the change in Coulomb stress along the Seattle fault (Fig. 1) due to a megathrust event. Using the Coulomb 2.0 software [22], we schematically model a Cascadia subduction earthquake scenario where the subduction thrust is represented by a series of rectangular faults, the earthquake slip is 20 m, and the regional stress field is such that $\sigma 1$ is horizontal N–S and $\sigma 3$ is vertical [4]. This model indicates a rather large variability of the Coulomb stress change with the Seattle-fault dip, depth, and friction coefficient. For most of these parameter combinations, the Coulomb stress for a thrust event on the Seattle fault increases by 0.01–0.1 MPa, confirming a possible triggering of a Seattle-fault earthquake by a subduction event.

Acknowledgements

We thank Tom James for his help with the ITRF transformations. This manuscript benefited

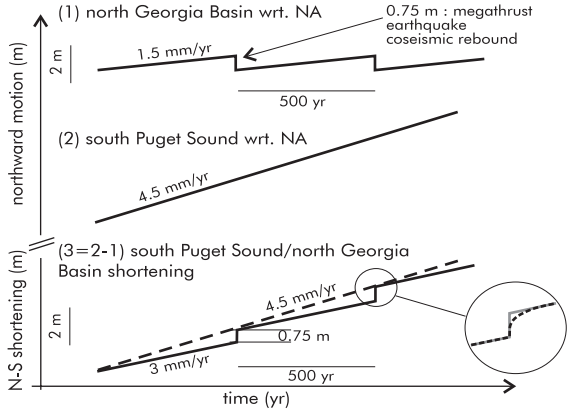

Fig. 6. Evolution of N–S shortening in the Puget–Georgia basin. Solid lines show the total motion (long-term+subduction-related transient) of points in northern Georgia Basin (1) and southern Puget Sound (2), and the shortening between these two points (3). Dashed line (3) shows the average long-term shortening.

from constructive reviews by Lucy Flesch, Jeff Freymueller, Garry Rogers and an anonymous reviewer. Figures were prepared using the Generic Mapping Tool software [23]. This research was partly supported by the Canadian GEOIDE network. Geological Survey of Canada Contribution number 2001036.*[AC]*

References

[1] R.E. Wells, C.S. Weaver, R.J. Blakely, Forearc migration in Cascadia and its neotectonics significance, Geology 26 (1998) 759–762.

[2] R. McCaffrey, C.K. Johnson, P.C. Zwick, M.D. Long, C. Goldfinger, J.L. Nabelek, C. Smith, Rotation and plate locking along the southern Cascadia subduction zone, Geophys. Res. Lett. 21 (2000) 3117–3120.

[3] S.Y. Johnson, C.J. Potter, J.M. Armentrout, Origin and evolution of the Seattle fault and Seattle basin, Geology 22 (1994) 71–74.

[4] K. Wang, T. Mulder, G.C. Rogers, R.D. Hyndman, Case for very low coupling stress on the Cascadia subduction fault, J. Geophys. Res. 100 (1995) 12907–12918.

[5] S. Mazzotti, P. Henry, X. Le Pichon, Transient and permanent deformation of central Japan estimated by GPS. 2. Strain partitioning and arc–arc collision, Earth Planet. Sci. Lett. 184 (2001) 455–469.

[6] M. Bevis, E. Kendrick, R. Smalley, B.A. Brooks, R.W. Allmendinger, B.L. Isacks, On the strength of interplate coupling and the rate of back-arc convergence in the central Andes: An analysis of the interseismic velocity field, Geochem. Geophys. Geosyst. 2 (2001) 10.129/2001GC000198.

[7] M.M. Miller, D.J. Johnson, C.M. Rubin, H. Dragert, K. Wang, A. Qamar, C. Goldfinger, GPS determination of along-strike variations in Cascadia margin kinematics: Implications for relative plate motion, subduction zone coupling, and permanent deformation, Tectonics 20 (2001) 161–176.

[8] H. Dragert, X. Chen, J. Kouba, GPS monitoring of crustal strain in southwest British Columbia with the Western Canada Deformation Array, Geomatica 49 (1995) 301–313.

[9] J.A. Henton, H. Dragert, R. McCaffrey, K. Wang, R.D. Hyndman, GPS monitoring of deformation at the northern Cascadia subduction zone, EOS Trans. AGU 81 (2000) F328.

[10] C. DeMets, T.H. Dixon, New kinematic models for the Pacific-North America motion from 3 Ma to present, I: Evidences for steady motion and biases in the NUVEL-1A model, Geophys. Res. Lett. 26 (1999) 1921–1924.

[11] J.C. Savage, M. Lisowski, W.H. Prescott, Strain accumulation in western Washington, J. Geophys. Res. 96 (1991) 14493–14507.

[12] R.D. Hyndman, K. Wang, The rupture zone of Cascadia great earthquakes from current deformation and the thermal regime, J. Geophys. Res. 100 (1995) 22133–22154.

[13] J.C. Savage, A dislocation model of strain accumulation and release at a subduction zone, J. Geophys. Res. 88 (1983) 4984–4996.

[14] P. Flück, R.D. Hyndman, K. Wang, Three-dimensional dislocation model for great earthquakes of the Cascadia subduction zone, J. Geophys. Res. 102 (1997) 20539–20550.

[15] D.S. Wilson, Confidence intervals for motion and deformation of the Juan de Fuca plate, J. Geophys. Res. 98 (1993) 16053–16071.

[16] C. DeMets, R.G. Gordon, D.F. Argus, S. Stein, Effect of recent revisions to the geomagnetic reversal time scale on estimates of current plate motions, Geophys. Res. Lett. 21 (1994) 2191–2194.

[17] K. Wang, R.E. Wells, S. Mazzotti, R.D. Hyndman, A revised dislocation model of interseismic deformation of the Cascadia subduction zone, J. Geophys. Res. (2002) submitted.

[18] G. Khazaradze, A. Qamar, H. Dragert, Tectonic deformation in western Washington from continuous GPS measurements, Geophys. Res. Lett. 26 (1999) 3153–3156.

[19] R.D. Hyndman, S. Mazzotti, D.H. Weichert, G.C. Rogers, Large earthquake rate of occurrence in Puget Sound–S. Georgia Strait predicted from geodetic and geological deformation rates, J. Geophys. Res. (2002) submitted.

[20] R.E. Well, R.W. Simpson, Northward migration of the Cascadia forearc in the northwestern US and implications for subduction deformation (abstract), PANGA Annual Meet. (2000) Corvalis, OR.

[21] S.K. Pezzopane, R.J. Weldon, Tectonic role of active faulting in central Oregon, Tectonics 12 (1993) 1140–1169.

[22] S. Toda, R.S. Stein, P.A. Reasenberg, J.H. Dieterich, Stress transferred by the Mw = 6.5 Kobe, Japan, shock: Effect on aftershocks and future earthquake probabilities, J. Geophys. Res. 103 (1998) 24543–24565.

[23] P. Wessel, W.H.F. Smith, New improved version of Generic Mapping Tools released, EOS Trans. AGU 79 (1998) F579.